Comparative studies of low-order and low-degree solar p modes

T.Appourchaux[1], B.Andersen[2], W.Chaplin[3], Y.Elsworth[3], W.Finsterle[4], C.Fröhlich[4], D.O.Gough[5], T.Hoeksema[6], G.Isaak[3], A.Kosovichev[6], J.Provost[7], P.Scherrer[6], T.Sekii[5], T.Toutain[7]

[1]Space Science Department of ESA, ESTEC, NL-2200 AG Noordwijk, (thierrya@so.estec.esa.nl)
[2]Norwegian Space Centre, N-0212 Oslo
[3]School of Physics and Astronomy, University of Birmingham
[4]Physikalisch-Meterologisches Observatorium World Radiation Center, CH-7260 Davos Dorf
[5]Institute of Astronomy, University of Cambridge, Cambridge CB3 0HA, UK
[6]W.W. Hansen Experimental Physics Laboratory, Stanford University, Stanford CA 94305
[7]Departement Cassini, URA CNRS 1362, Observatoire de la Côte d'Azur, F-06304 Nice

ABSTRACT

The amplitudes of solar p modes decrease steeply with decreasing radial order below about 17. The background solar signal (solar noise) in general increases steadily with decreasing frequency. For the irradiance and radianace measurements with VIRGO or SOI/MDI on SOHO, this combination makes it difficult to detect low degree modes below about 1.8 mJz. The solar noise as oberverved in velocity with SOI/MDI or the ground based BiSON network is significantly lower in this region than in intensity measurements. This permits low-degree modes to be observed close to 1 mHz.

We present results of detection and characterization of the lowest-order observable p modes both in velocity and intensity measurements. Where applicable the properties of the modes observed with the two methods are compared.

Key words: p modes - low order - Sun

1. Introduction

The low-frequency p modes do not penetrate as deeply as the high-frequency modes, but because of their smaller linewidths, their frequencies are expected to be measured more precisely. These precise frequencies would provide us with strong constraints on the physical condition of the solar core. Detection of low-frequency p modes was reported by Chaplin et al.(1996) who used 32 months of BiSON data. They claimed detection of modes down to $n = 7$. Lazrek et al.(1997), using the GOLF data on board SOHO, confirmed the detection of the modes down to $n = 8$.

In 1997, the Phoebus working group was set up for detecting g modes (Appourchaux, these proceedings). The strategy of the group was to test g-mode detection techniques on low-frequency p modes. Here we present our findings. In the next section, we list the data we used. In the subsequent section, we discuss the results obtained for the frequencies and linewidths.

2. The time series

The data analysed are the following:

- Full-disk integrated instruments:
  - -BiSON: 32-month velocity data (starting 1994 Jan 1)
  - -VIRGO/SPM: 713 days of intensity data (starting 1996 May 1)
- Imaging instruments:
  - -SOI/MDI: 610 days of velocity data (starting 1996 May 1)
  - -VIRGO/LOI: 733 days of intensity data (starting 1996 March 27)

The data from BiSON are reduced as in Chaplin et al.(1997a) and Elworsth et al.(1995). The VIRGO/SPM data are reduced as in Fröhlich et al.(1997). The SOI/MDI data are reduced as in Toutain et al.(1998). The VIRGO/LOI data reduction is described by Appourchaux and the VIRGO team (these proceedings).

3. Results

Figures 1 and 2 show regular echelle diagrams for BiSON and SOI/MDI (On the CD-ROM supplement, see file `mmm/anders_3/figure1.ps` and `mmm/anders_3/figure2.ps`). The signal-to-noise ratio is better for SOI/MDI at low frequency owing to a better window function and instrumental homogeneity. For detecting low-frequency p modes, we have used the collapsogram technique described by Appourchaux (these proceedings). Figures 3 and 4 show echelle diagrams of collapsograms for the LOI and SOI/MDI (On the CD-ROM supplement, see file `mmm/anders_3/figure3.ps` and `mmm/anders_3/figure4.ps`). The LOI collapsogram does not help to bring out modes that are resolved, e.g. when the mode lifetime is shorter than the observing time. For instance, the MDI collapsogram helps us to 'see' modes for very low n for which the mode lifetime is longer than the observation time. Figures 5 to 7 show the collapsogram spectra around the $l = 1$ modes of $n = 6, 7$ and 8 respectively. The identification of the modes is not always unambiguous.

After identifying the modes, we have fitted the data for extracting the frequencies and linewidths of the modes. The data were fitted using Maximum-Likelihood Estimation on the power spectra for the BiSON and VIRGO/SPM data, and on Fourier spectra for the SOI/MDI and LOI data. (For a review of fitting techniques, see Appourchaux, these proceedings.) For power spectra, a common amplitude and linewidth is fitted to a multiplet, only the ratio between the $|m|$ is fixed. The assumed line profile is a Lorentzian. Tables 1,2 and 3 give the frequencies measured by the different instruments for $l = 0, 1$ and 2, respectively. Figure 8 gives the linewidths measured by the velocity instruments for the low-frequency modes (On the CD-ROM supplement, see file `mmm/anders_3/figure8.ps`). As shown by Toutain et al.(1997), the frequencies measured by intensity instruments are systematically higher than those of velocity

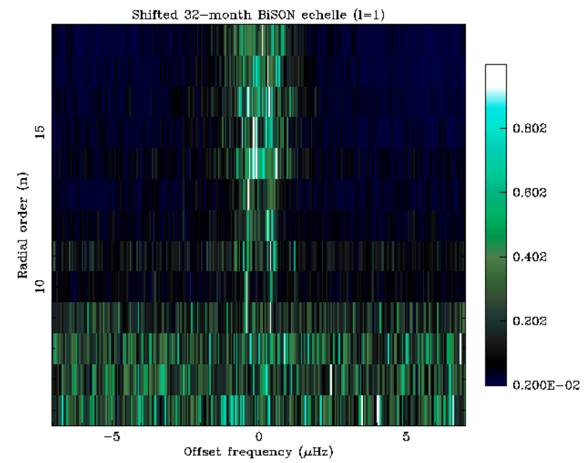

Figure 1: Echelle diagram of the l=1 modes for 32 months of BiSON data. The diagram is constructed by using theoretical frequencies for each n. The data are normalized by the maximum power in each n. The pair of l=1 modes are clearly visible down to n=9.

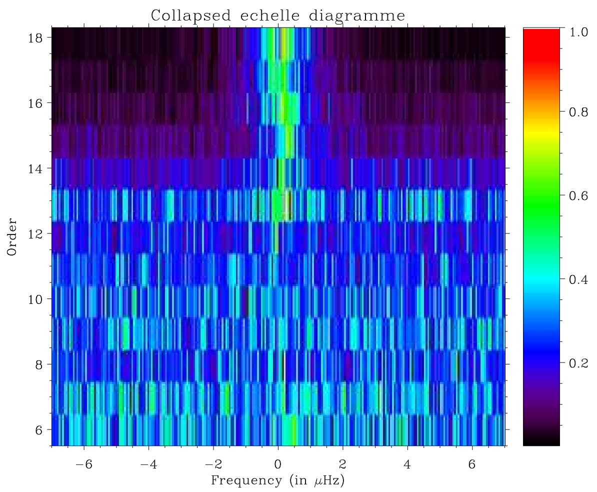

Figure 3: Echelle diagram of collapsogram of l=1 for 733 days of LOI data using theoretical frequencies for each n. The splitting used for shifting is about 412 nHz.

instruments. This is a results of the p-mode line profiles having different asymmetry in velocity and intensity (Nigam et al., these proceedings). You may notice some discrepancy between the fitted frequencies and the locations of the peaks for $l = 1$, $n = 7$; this exemplifies the diffciulties of fitting data for which the profile of the modes is not resolved. From 8, we can deduce that an integration time of about 10 years may be required for resolving the $l = 1$, $n = 6$.

4. Conclusion

We have reported on the frequencies of the lowest order p modes detected so far. A preliminary frequency comparison shows that frequencies derived from intensity measurements are higher than those of intensity measurements. An observation of time of about 10 years could

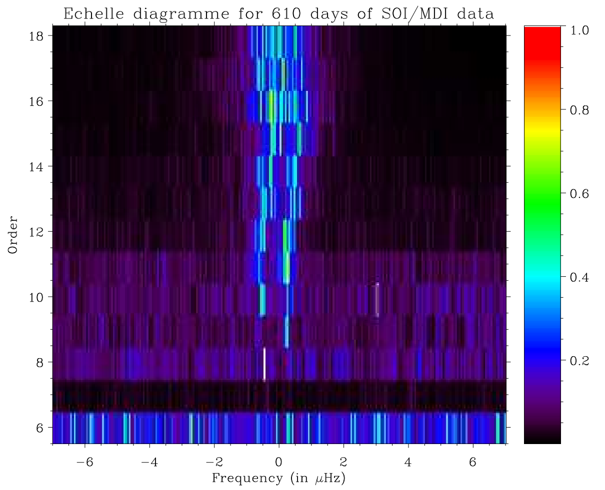

Figure 2: Echelle diagram of l=1, $|m|$=1, for 610 days of SOI/MDI data using theoretical frequencies for each n. The diagram is constructed by using theoretical frequencies for each n. The data are normalized by the maximum power in each n. Pair of l=1 modes are clearly visible down to n=8. The improvement over the BiSON data comes from the absence of atmospheric noise.

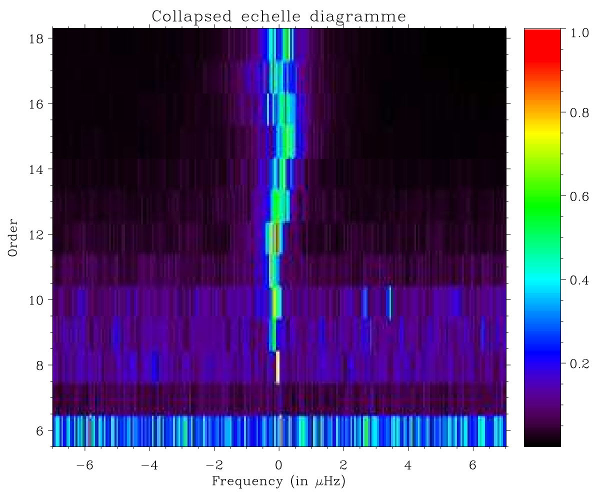

Figure 4: Echelle diagram of collapsogram of l=1 for 610 days of SOI/MDI data using theoretical frequencies for each n. The splitting used for shifting is about 412 nHz. Mode down to n=6 can be detected (i.e. at about 1039 microHz).

be required for resolving the lowest mode frequencies by the techniques we have adopted.

Acknowledgements

SOHO is a project of international collaboration between ESA and NASA. BiSON is supported by the UK Particle Physics Astronomy Research Council.

References

Appourchaux, T., Andersen, B. N., Frohlich, C., Jimenez, A., Telljohann, U., & Wehrli, C. 1997, Sol. Phys., 170, 27

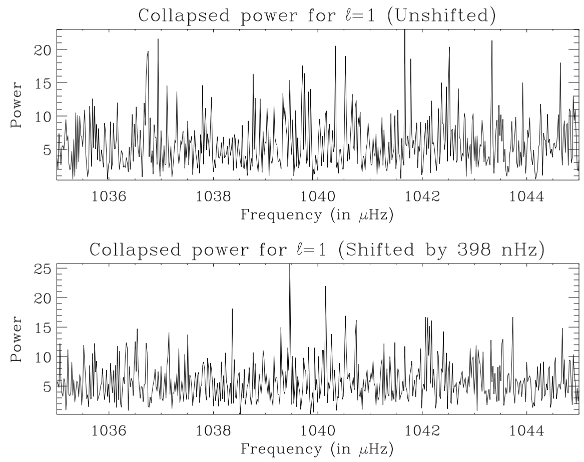

Figure 5: Collapsogramme of l=1 for 610 days of SOI/MDI data, unshifted (top) and shifted (bottom). The probability that the peak at 1039.5 μHz is due to noise is 0.12. This is a possible identification of the $l = 1$, $n = 6$ mode.

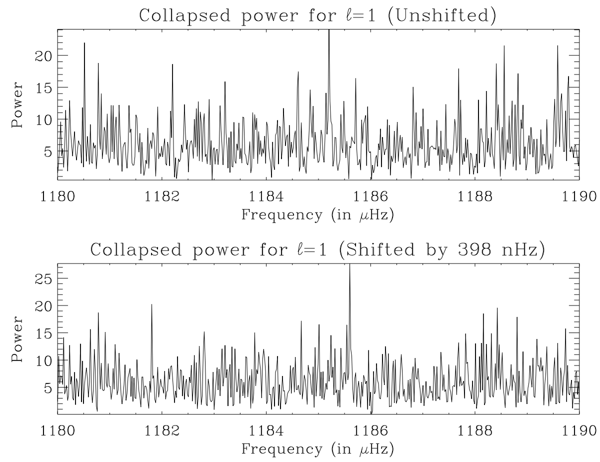

Figure 6: Collapsogramme of l=1 for 610 days of SOI/MDI data, unshifted (top) and shifted (bottom). The probability that the peak at 1329.4 μHz is due to noise is 0.05. This is a possible identification of the $l = 1$, $n = 7$ mode.

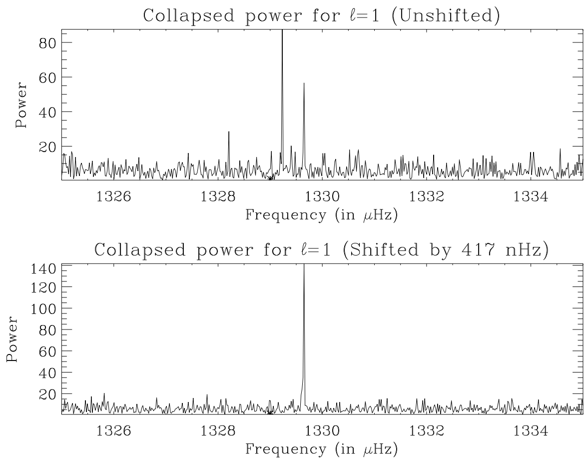

Figure 7: Collapsogramme of l=1 for 610 days of SOI/MDI data, unshifted (top) and shifted (bottom). The probability that the peak at 1329.6 μHz is due to noise is less than $3\ 10^5$. This is clearly the identification of the $l = 1$, $n = 8$ mode.

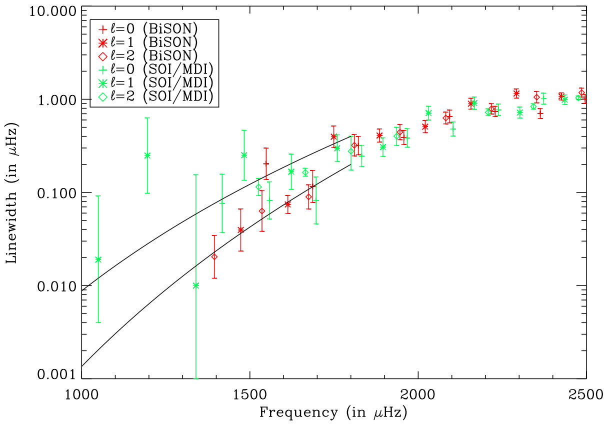

Figure 8: Linewidth of the low-frequency p modes as a function of frequency measured by BiSON (Red or black) and SOI/MDI (Green or grey). Note that the identification of the 2 lowest $l = 1$ modes is doubtful and that their linewidth may not be realistic. The two continuous black lines are the 1-σ upper amd lower limits as derived from Chaplin et al.(1996), assuming a power law dependence of the linewidth upon frequency (α=7 $\pm$ 1.5. At around 1mHz, the predicted lifetime ($1/\Gamma$) is longer than 10 years.

Chaplin, W. J., Elsworth, Y., Howe, R., Isaak, G. R., McLeod, C. P., Miller, B. A., & New, R. 1997a, A&ASup. Series, 125, 195

Chaplin, W. J., Elsworth, Y., Isaak, G. R., Lines, R., McLeod, C. P., Miller, B. A., New, R. 1996, MNRAS, 282, L15

Chaplin, W. J., Elsworth, Y., Isaak, G. R., McLeod, C. P., Miller, B. A., & New, R. 1997b, MNRAS, 288, 623

Fröhlich, C., Andersen, B. N., Appourchaux, T., Berthomieu, G., Crommelynck, D. A., Domingo, V., Fichot, A., Finsterle, W., Gomez, M. F., Gough, D., Jimenez, A., Leifsen, T., Lombaerts, M., Pap, J. M., Provost, J., Cortes, T. R., Romero, J., Roth, H., Sekii, T., Telljohann, U., Toutain, T., & Wehrli, C. 1997, Sol. Phys., 170, 1

Elsworth, Y., Howe, R., Isaak, G. R., McLeod, C. P., Miller, B. A., New, R., Wheeler, S. J. 1995, A&ASup. Series, 113, 379

Lazrek, M., Baudin, F., Bertello, L., Boumier, P., Charra, J., Fierry-Fraillon, D., Fossat, E., Gabriel, A. H., Garcia, R. A., Gelly, B., Gouiffes, C., Grec, G., Pallé, P. L., Hernandez, F. P., Régulo, C., Renaud, C., Robillot, J. -M., Cortés, T. R., Turck-Chièze, S., & Ulrich, R. K. 1997, Sol. Phys., 175, 227

Toutain, T., Appourchaux, T., Baudin, F., Froehlich, C., Gabriel, A., Scherrer, P., Andersen, B. N., Bogart, R., Bush, R., Finsterle, W., Garcia, R. A., Grec, G., Henney, C. J. , Hoeksema, J. T., Jimenez, A., Kosovichev, A., Cortes, T. R., Turck-Chieze, S., Ulrich, R., Wehrli, C. 1997, Sol. Phys., 175, 311

Toutain, Kosovichev, A. G.. & Appourchaux, T. 1997, IAU Symposia, 185, E54

Table 1: l=0 frequencies for the Phoebus data and their 1-σ error bars.

n	SPM blue	SPM green	SPM red	LOI	BiSON	SOI/MDI
9	-	-	-	-	-	1407.454 $\pm$ 0.021
10	-	-	-	-	1548.328 $\pm$ 0.037	1548.294 $\pm$ 0.017
11	-	-	-	-	1686.590 $\pm$ 0.017	1686.564 $\pm$ 0.018
12	-	-	-	-	1822.157 $\pm$ 0.031	1822.181 $\pm$ 0.030
13	1957.545 $\pm$ 0.048	1957.559 $\pm$ 0.054	1957.568 $\pm$ 0.057	1957.594 $\pm$ 0.066	1957.381 $\pm$ 0.032	1957.353 $\pm$ 0.037
14	2093.571 $\pm$ 0.070	2093.565 $\pm$ 0.068	2093.591 $\pm$ 0.053	2093.567 $\pm$ 0.068	2093.513 $\pm$ 0.042	2093.437 $\pm$ 0.038
15	2228.780 $\pm$ 0.078	2228.808 $\pm$ 0.065	2228.824 $\pm$ 0.065	2228.720 $\pm$ 0.083	2228.634 $\pm$ 0.042	2228.663 $\pm$ 0.048
16	2362.889 $\pm$ 0.059	2362.872 $\pm$ 0.062	2362.904 $\pm$ 0.062	2362.875 $\pm$ 0.069	2362.790 $\pm$ 0.036	2362.749 $\pm$ 0.056
17	2496.288 $\pm$ 0.060	2496.292 $\pm$ 0.059	2496.330 $\pm$ 0.059	2496.295 $\pm$ 0.069	2496.116 $\pm$ 0.047	2496.100 $\pm$ 0.051

Table 2: l=1 frequencies for the Phoebus data and their 1-σ error bars. Doubtful identification of modes are in parentheses.

n	SPM blue	SPM green	SPM red	LOI	BiSON	SOI/MDI
6	-	-	-	-	-	(1039.463 $\pm$ 0.014)
7	-	-	-	-	-	(1185.336 $\pm$ 0.185)
8	-	-	-	-	-	1329.649 $\pm$ 0.010
9	-	-	-	-	1472.826 $\pm$ 0.008	1472.871 $\pm$ 0.089
10	-	-	-	-	1612.715 $\pm$ 0.009	1612.705 $\pm$ 0.019
11	-	-	-	-	1749.254 $\pm$ 0.052	1749.242 $\pm$ 0.020
12	-	-	-	-	1885.084 $\pm$ 0.030	1885.068 $\pm$ 0.018
13	2021.017 $\pm$ 0.050	2021.024 $\pm$ 0.050	2021.029 $\pm$ 0.045	2020.958 $\pm$ 0.054	2020.780 $\pm$ 0.029	2020.745 $\pm$ 0.022
14	2156.855 $\pm$ 0.059	2156.869 $\pm$ 0.080	2156.853 $\pm$ 0.066	2156.942 $\pm$ 0.059	2156.679 $\pm$ 0.043	2156.745 $\pm$ 0.025
15	2292.124 $\pm$ 0.039	2292.128 $\pm$ 0.038	2292.153 $\pm$ 0.038	2292.044 $\pm$ 0.039	2291.890 $\pm$ 0.042	2291.910 $\pm$ 0.024
16	2425.605 $\pm$ 0.067	2425.613 $\pm$ 0.065	2425.672 $\pm$ 0.070	2425.660 $\pm$ 0.034	2425.559 $\pm$ 0.056	2425.454 $\pm$ 0.026

Table 3: l=2 frequencies for the Phoebus data and their 1-σ error bars.

n	SPM blue	SPM green	SPM red	LOI	BiSON	SOI/MDI
8	-	-	-	-	1394.659 $\pm$ 0.008	1394.650 $\pm$ 0.010
9	-	-	-	-	1535.857 $\pm$ 0.012	1535.795 $\pm$ 0.037
10	-	-	-	-	1674.536 $\pm$ 0.010	1674.531 $\pm$ 0.011
11	-	-	-	-	1810.287 $\pm$ 0.037	1810.265 $\pm$ 0.014
12	1945.844 $\pm$ 0.038	1945.794 $\pm$ 0.085	1945.810 $\pm$ 0.062	1945.923 $\pm$ 0.073	1945.781 $\pm$ 0.034	1945.763 $\pm$ 0.016
13	-	2081.459 $\pm$ 0.262	-	2082.189 $\pm$ 0.048	2081.929 $\pm$ 0.046	2082.067 $\pm$ 0.018
14	2217.641 $\pm$ 0.199	2217.471 $\pm$ 0.224	2217.348 $\pm$ 0.157	2217.804 $\pm$ 0.037	2217.622 $\pm$ 0.056	2217.606 $\pm$ 0.019
15	2352.351 $\pm$ 0.060	2352.332 $\pm$ 0.062	2352.350 $\pm$ 0.077	2352.314 $\pm$ 0.032	2352.088 $\pm$ 0.054	2352.184 $\pm$ 0.020
16	2485.994 $\pm$ 0.076	2486.009 $\pm$ 0.080	2485.983 $\pm$ 0.083	2485.988 $\pm$ 0.031	2485.737 $\pm$ 0.058	2485.819 $\pm$ 0.022